



ELSEVIER

Journal of Alloys and Compounds 300–301 (2000) 45–54

Journal of  
ALLOYS  
AND COMPOUNDS

www.elsevier.com/locate/jallcom

# Simulation of the spectroscopic and magnetic properties of RE(III) ions in RE oxychlorides based on exact crystal structure from Rietveld refinements<sup>☆</sup>

Jorma Hölsä<sup>a,\*</sup>, Ralf-Johan Lamminmäki<sup>a,b</sup>, Mika Lastusaari<sup>a,b</sup>, Pierre Porcher<sup>c</sup>, Regino Sáez Puche<sup>d</sup>

<sup>a</sup>Department of Chemistry, University of Turku, FIN-20014 Turku, Finland

<sup>b</sup>Graduate School of Materials Research, Turku, Finland

<sup>c</sup>Laboratoire de Chimie Appliquée de l'Etat Solide, UMR 7574, CNRS, ENSCP, F-75231 Paris Cedex 05, France

<sup>d</sup>Departamento de Química Inorgánica I, Universidad Complutense, Ciudad Universitaria, E-28040 Madrid, Spain

## Abstract

The procedures to calculate the  $4f^N$  energy level schemes — together with the related properties such as the paramagnetic susceptibility — of the trivalent rare earth ions ( $RE^{3+}$ ) in the tetragonal RE oxychlorides (REOCl, RE=La–Nd, Sm–Ho and Y) from structural data are presented. The methods include the determination of coherent and reliable structural parameters from X-ray powder diffraction measurements using Rietveld analyses. The measurement of the absorption and luminescence spectra of the  $RE^{3+}$  ions from the IR to UV region yield the experimental  $4f^N$  energy level schemes which are then simulated with a phenomenological model involving the parametrization of the inter- and intra-ionic interactions. Parallel calculations — already proven to be successful for ionic systems such as RE oxyfluorides — are based on the modified point charge model (PCEM). The more covalent simple overlap (SOM) model is also applied and compared to the other results. Finally, the paramagnetic susceptibility of the pure oxychlorides as a function of temperature was calculated using the eigenfunctions and eigenvalues from the phenomenological simulation of the experimental  $4f^N$  energy level schemes. © 2000 Elsevier Science S.A. All rights reserved.

**Keywords:** X-ray powder diffraction; Rietveld profile refinement; Energy level schemes; Paramagnetic susceptibility; Rare earth oxychlorides

## 1. Introduction

The  $RE^{3+}$  doped tetragonal rare earth oxychlorides (REOCl) are efficient luminescent materials and have thus been exploited in many industrially important applications for a number of years [1]. The oxyhalide matrix is interesting from the theoretical point of view, too, because of the simple but high-symmetry crystal structure [2]. However, the structural data reported earlier for almost all tetragonal oxychlorides from LaOCl to HoOCl are rather incoherent [2–11]. This is most probably because of different experimental setups and data treatment proce-

dures utilized. Also the treatment of the X-ray and/or neutron powder diffraction data is inherently complicated with theoretical and, most of all, practical difficulties. The structural data available are clearly unsuitable for use in accurate theoretical calculations.

In contrast to the structural data, the optical absorption and luminescence spectra of the  $RE^{3+}$  doped RE oxychlorides have been studied in detail [12–20]. The experimental energy level schemes obtained by simulations based on the phenomenological model took simultaneously account of both the free ion and crystal field (c.f.) effects. The good agreement between the calculated and experimental energy level schemes yielded accurate wave functions associated with each level. These simulations enable the calculation of other physical properties of the  $RE^{3+}$  ions, such as the temperature dependence of the paramagnetic susceptibility, which have not yet been studied to any extent in the REOCl matrices.

The aim of this paper is to present the results of

<sup>☆</sup>Presented at the 3rd International Winter Workshop on Spectroscopy and Structure of Rare Earth Systems, Szklarska Poręba/Wrocław, Poland, April 27–May 1, 1999.

\*Corresponding author. Tel.: +358-2-333-6737; fax: +358-2-333-6730.

E-mail address: jholsa@utu.fi (J. Hölsä)

multidisciplinary investigations combining extensive experimental and theoretical work on both the structural and physical properties of the RE oxychlorides extending over a considerable number of years and researchers. The final goal of these contributions is to develop a theoretical model that is easy to use and has wide applicability to different RE systems.

## 2. Experimental

### 2.1. Sample preparation

The polycrystalline rare earth oxychlorides REOCl (RE=La–Ho and Y but excluding Pm) were prepared using a solid-state reaction between the corresponding RE oxides and ammonium chloride intimately mixed [21]. The purity and structure of the samples was routinely verified with the X-ray powder diffraction analyses but no anomalies were observed.

### 2.2. X-ray powder diffraction and Rietveld analysis

The X-ray powder diffraction patterns of REOCl were collected using an Enraf-Nonius PDS120 diffractometer using an INEL CPS120 position-sensitive detector. The measurements were carried out at room temperature between 5 and 125° in  $2\theta$  with  $\text{CuK}\alpha_1$  radiation ( $\lambda=1.54060$  Å) and a flat rotating sample holder. The data collecting times were 90 (TbOCl, DyOCl, and HoOCl) or 75 min for the remaining REOCl samples. A mixture of silicon (NIST Standard 640b) and fluorophlogopite (NIST Standard 675) powders were used as an external standard. The resolution of the apparatus was better than 0.018° in  $\theta$ .

The diffraction data between 20 and 110° were analyzed using the Rietveld profile refinement method using the FullProf program V3.2 (January 1997). The parameters refined were as follows (in the order of introduction to the refinement):  $2\theta$  zero-point correction, background (a fifth-order polynomial function), scale factor, unit cell parameters  $a$  and  $c$ , fractional atomic coordinates, pseudo-Voigt half-width parameters  $U$ ,  $V$  and  $W$ , peak asymmetry parameter, profile shape parameter, and isotropic temperature factors  $B$ . Also the microabsorption and preferred orientation corrections had to be applied.

### 2.3. Spectroscopic measurements

The optical absorption spectra of REOCl powder samples were obtained in the NIR, visible and UV ranges at selected temperatures between 9 and 300 K in the wavelength range 200–3000 nm (50 000–3333  $\text{cm}^{-1}$ ). Standard KBr pellet techniques were used for the sample preparation.

The luminescence spectra of the REOCl:RE<sup>3+</sup> (RE=La and Gd) powder samples were measured usually at 77 and

300 K under Ar<sup>+</sup>-ion laser or mercury lamp excitation and detected using a 1-m monochromator with photomultiplier detection connected with standard electronics. More experimental details on optical measurements can be found in Refs. [12,16,19,20].

### 2.4. Simulation of energy level schemes

The simulation of the 4f<sup>N</sup> energy level schemes of the RE<sup>3+</sup> ions in REOCl were carried out by considering simultaneously both the free ion and c.f. interactions. In this parametrization scheme each interaction was described by one or more parameters [22]. The free ion interactions included the electrostatic electron repulsion (Racah parameters  $E_k$ ;  $k=0, 1, 2, 3$ , or Slater integrals  $F^k$ ;  $k=0, 2, 4, 6$ ) and spin-orbit coupling (the coupling constant  $\zeta_{4f}$ ) terms. The two- and three-body configuration interactions were included with the Trees ( $\alpha$ ,  $\beta$  and  $\gamma$ ) and Judd  $T^k$  ( $k=2, 3, 4, 6, 7$  and  $8$ ) parameters, respectively [23,24] [Eq. (1)]:

$$H = \sum_{k=0}^3 E_k(nf, nf)e^k + \zeta_{4f}A_{SO} + \alpha L(L+1) + \beta G(G_2) + \gamma G(G_7) + \sum_{k=2,3,4,6,7,8} T^k t_k \quad (1)$$

The relativistic spin-spin and spin-other-orbit interactions of minor importance were neglected. The whole 4f<sup>N</sup> configurations were used in all calculations in contrast to most studies which have employed more or less extensive truncations.

The c.f. effect accounted for in the simulations included only the standard one-electron concept since there has been no indication that the inclusion of the two-electron part improves the simulation of the lower levels. Following Wybourne's [23] formalism [Eq. (2)], the c.f. Hamiltonian was expressed as a sum of products between the spherical harmonics  $C_q^k$  and the c.f. parameters  $B_q^k$ . The number of non-zero c.f. parameters is five ( $B_0^2, B_0^4, B_4^4, B_0^6$  and  $B_4^6$ ) for the  $C_{4v}$  symmetry of the RE<sup>3+</sup> site in RE oxychlorides:

$$H_{c.f.} = \sum_k \sum_{q=-k}^{q=k} \{ B_q^k [ C_q^k + (-1)^q C_{-q}^k ] + i S_q^k [ C_q^k - (-1)^{-q} C_{-q}^k ] \} \quad (2)$$

### 2.5. Paramagnetic susceptibility

The magnetic susceptibility of the REOCl powder samples (ca. 10 mg) was measured between 2 and 200–300 K with a Quantum Design SQUID MPMS-XL magnetometer applying a magnetic field of 1000 Oe. The experimental susceptibility values were corrected against the diamagnetic contribution of the RE<sup>3+</sup>, O<sup>2-</sup> and Cl<sup>-</sup> ions. For the RE compounds the difference between the experimental paramagnetic susceptibility and that predicted

by the Curie–Weiss law,  $\chi = C/(T - \theta)$ , at low temperatures is generally due to the c.f. effect which can be accounted for by the van Vleck formula [25] [Eqs. (3) and (4)]:

$$\chi = N_A \beta^2 \sum_i \left( \frac{\langle \Phi_i | \mu | \Phi_i \rangle^2}{kT} - 2 \sum_{j \neq i} \frac{\langle \Phi_i | \mu | \Phi_j \rangle \langle \Phi_j | \mu | \Phi_i \rangle}{E_i - E_j} \right) \beta_i \quad (3)$$

where:

$$\beta_i = \frac{\exp(-E_i/kT)}{\sum_i d_i \exp(E_i/kT)} \quad (4)$$

where  $\beta_i$  is the Boltzmann thermal population coefficient of the energy levels, and  $N_A$ ,  $\beta$ ,  $\phi_i$  and  $E_i$  are the Avogadro constant, the Bohr magneton, and the non-perturbed wave functions, as well as the energies of the energy levels in the absence of a magnetic field, respectively. The wave functions  $\phi_i$  and energy level values  $E_i$  were provided by the level simulations of the RE<sup>3+</sup> ions in the REOCl hosts (Section 2.4). The degeneracy of the energy levels is given by the term  $d_i$ .

The magnetic moment tensor operator is  $\mu = (L + g_e S)$ . The magnetic anisotropy to be observed only for an ion in a site of symmetry lower than cubic is caused by the non-equal components, i.e.  $\chi_{\perp}$  ( $\pm 1$ ) and  $\chi_{\parallel}$  (0 component), of the paramagnetic susceptibility. However, only the mean susceptibility  $\langle \chi \rangle = [2\chi_{\perp} + \chi_{\parallel}]/3$  can be measured for powders.

### 3. Theoretical models

#### 3.1. Electrostatic point charge model

The point charge model uses the simplest description of the c.f. concept neglecting all but the point charge effects. In the modified electrostatic point charge model (PCEM), however, the inadequacies of the basic model are partly compensated by some empirical correction factors. According to this model the c.f. parameters can be expressed as follows [26]:

$$B_q^k = \tau^{-k} (1 - \sigma_k) A_q^k \langle r^k \rangle \quad (5)$$

PCEM thus allows the parameters to be split into the electrostatic lattice sum parameters  $A_q^k$  [27] and the free ion radial integrals  $\langle r^k \rangle$ , which depend only on the host lattice and the doping ion, respectively. The radial integrals are subject to two corrections [26]: the factors  $\tau$  and  $\sigma_k$  describe the expansion of the 4f wave functions in the solid state and the shielding effect of the 5s, 5d and 5p electrons, respectively. The expansion factor,  $\tau$ , and the shielding factor,  $\sigma_2$ , for each RE<sup>3+</sup> dopant were obtained from linear extrapolation as a function of the number of the 4f electrons. The  $\sigma_4$  and  $\sigma_6$  values were taken as

constants in the whole RE<sup>3+</sup> series. The Dirac–Fock values [28] for the  $\langle r^k \rangle$  radial integrals were used instead of the more conventional Hartree–Fock values.

The lattice sum parameters need also a modification of the charges of the ions since both the structural (electron density distribution) and spectroscopic (XPS) [29] investigations have shown that the nominal charges (RE, +3; O, -2; Cl, -1) are not realistic ones. The effective charge +1.5 used for all RE<sup>3+</sup> ions is close to the value found for yttrium in Y<sub>2</sub>O<sub>3</sub> (+1.6–1.7) [29]. The charges of O (-1.0) and Cl (-0.5) were then chosen to meet the requirements of the stoichiometry and the zero total charge of REOCl.

#### 3.2. Simple overlap model

The basic idea of the Simple Overlap Model (SOM) is similar to that of the modified point charge model [30]. The difference between SOM and PCEM lies in the fact that the potential experienced by the 4f electrons due to the neighbouring ions is supposed to be equivalent to that created by charges uniformly distributed in a small region around the centre of the metal–ligand distance [31]. The total charge of a region is given by the product between the charge and the overlap between the metal and the ligand orbitals. The overlap depends on the type and the distance of the ligand from the metal. This can be written as a function of the shortest metal–ligand distance,  $R_0$ :

$$\rho_{\mu} = \rho_0 \left( \frac{R_0}{R_{\mu}} \right)^N, \quad \text{where } 2.5 < N < 5 \quad (6)$$

The c.f. parameters are then given by:

$$B_q^k = \langle r^k \rangle \sum \rho_{\mu} \left( \frac{2}{1 \pm \rho_{\mu}} \right)^{k+1} A_q^k(\mu) \quad (7)$$

The sum  $\mu$  runs over all the ions in the first coordination sphere.  $A_q^k$  are the lattice sums taking into account only the neighbouring anions and include also the effective charges similar to PCEM. The  $\langle r^k \rangle$  are the Dirac–Fock radial integrals [28].

The effective charges of the ions, the overlap,  $\rho$ , and the exponent,  $N$ , were modified in a manner to find the best agreement between the calculated and phenomenological c.f. parameters. The effective charges -0.9 and -0.8 were used for the chloride and oxide ions, respectively. The overlap parameter  $\rho$  values from 0.05 to 0.06 obtained indicate weak overlap, as expected for the rare earths ( $0.05 < \rho < 0.08$ ) [31] since the 4f orbitals are well protected by outer electron shells and participate only weakly in the bonding. The c.f. parameters are not sensitive to the exponent  $N$ , at least when it remains within the expected values ( $2.5 < N < 5$ ) [31]. The  $N$  was fixed to 3.5 for the REOCl series.

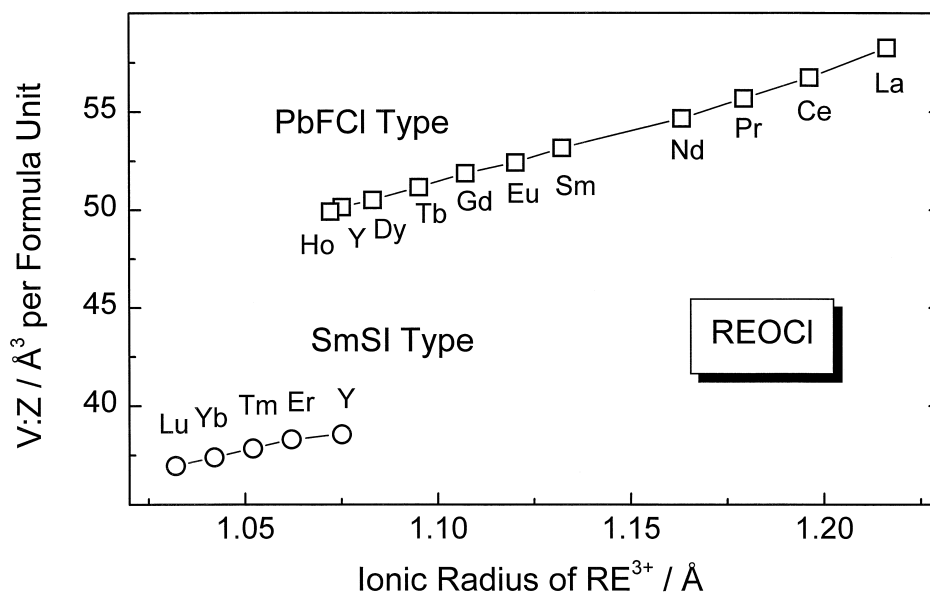


Fig. 1. Effect of the tetragonal to hexagonal phase transition on the (unit cell volume):  $Z$  value in the REOCl series.

## 4. Results and discussion

### 4.1. Crystal structure refinements

All the REOCl samples were found to possess the PbFCl-type tetragonal crystal structure with  $P4/nmm$  ( $Z=2$ ) as the space group [2] in contrast to TmOCl, YbOCl, LuOCl, and usually also ErOCl and YOCl which prefer the hexagonal SmSI- or YOF-type structure [32]. Although all three structural types are composed of alternating layers of  $(REO)_n^{n+}$  complex cations and  $Cl^-$  anions the volume occupied by the hexagonal REOCl unit is much smaller (Fig. 1) which results in the decreased stability of this form at ambient conditions.

The Rietveld refinements yielded good agreement between the experimental and calculated patterns as shown for LaOCl (Fig. 2). This was indicated by the low Bragg  $R$  ( $R_B$ ) values being all, except for EuOCl, lower than 10%. As far as the systematics and coherence of the results is concerned, the unit cell  $a$ - and  $c$ -axis lengths as well as the unit cell volume of the RE oxychlorides decrease linearly as the ionic radius of  $RE^{3+}$  host cation [33] decreases (Fig. 3), in contrast to the incoherent structural data reported earlier [2–11].

In order to achieve useful structural data for meaningful theoretical calculations the atomic positions are of utmost importance. In the tetragonal REOCl structure, the RE and chlorine atoms reside in the  $2c$  ( $1/4, 1/4, z$ ) positions

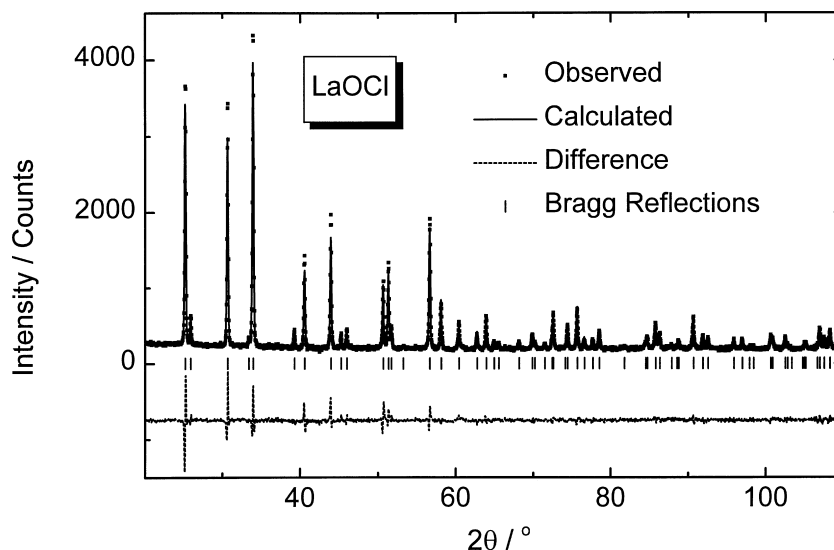


Fig. 2. Results of the Rietveld profile refinement of LaOCl.

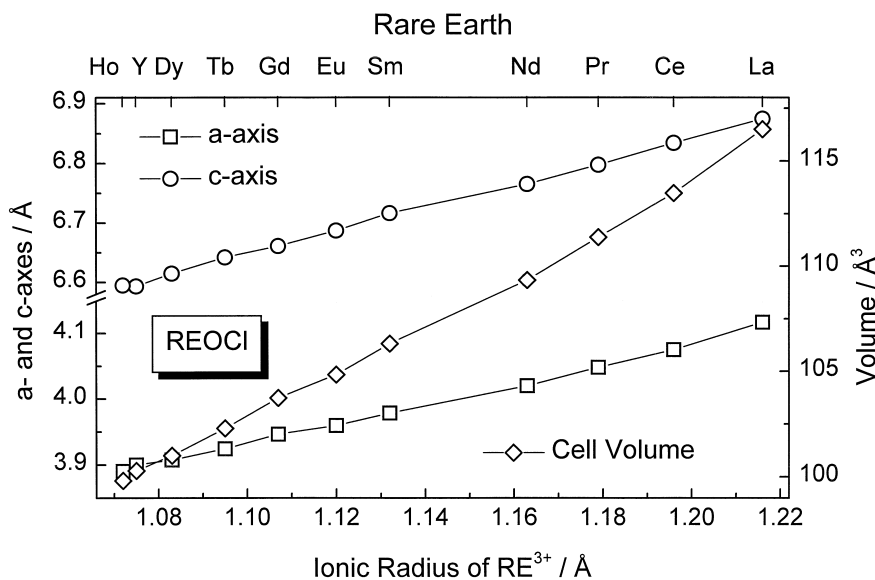


Fig. 3. Systematics in the REOCl series: unit cell dimensions. The E.S.D. values are smaller than the heights of the symbols.

[oxygens lie in  $2a(1/4, 3/4, 0)$ ] [2] which yields only two positional parameters to be refined. As a result of the Rietveld refinements, the  $z_{\text{RE}}$  coordinate decreases linearly from LaOCl to HoOCl, while  $z_{\text{Cl}}$  changes much less and achieves a local maximum at EuOCl. Due to the much lower number of electrons the chlorine position is inherently less precisely determined than the RE position but the results achieved must be considered satisfactory as indicated by the smooth variation of the bond distances. It should be noted that the present coherent results were obtained only by using the microabsorption and preferred orientation corrections, the effect of which was found invaluable.

The difficulties in achieving coherent structural data throughout the REOCl series is due to the different crystallinity of the samples. The crystallinity of the powder samples starts to increase beyond EuOCl due to repeated heating of the samples with  $\text{NH}_4\text{Cl}$ . This indicated that even if the sample-based effects are of little obvious significance when the structure of an individual compound is determined, they can not be neglected when a series of isostructural compounds is studied. Eventually, the Rietveld analyses of the room temperature X-ray powder diffraction patterns of the tetragonal RE (RE=La–Ho, and Y but excluding Pm) oxychlorides yielded a coherent and reliable set of structural parameters to be used in further theoretical calculations.

#### 4.2. Phenomenological simulation of energy level schemes

##### 4.2.1. Free ion effects

The simulation of the  $4f^N$  energy level schemes of the  $\text{RE}^{3+}$  ions in RE oxychlorides have been carried out successfully with satisfactory RMS deviations around 20

$\text{cm}^{-1}$  [12–20]. Further considerations have, however, shown that even better results can be obtained if some higher energy levels were excluded. This will be discussed in detail with the magnetic properties of the  $\text{RE}^{3+}$  ions. Recent results using a Hamiltonian which includes the magnetic spin–spin and spin–other-orbit interactions have shown that the importance of these terms is not insignificant after all [34] and the simulation of the higher energy level structure may be improved considerably.

The free ion parameters for the REOCl series reveal an obvious increase in the electrostatic interaction (the Racah parameters,  $E_k$ ) and in the spin–orbit coupling ( $\zeta_{4f}$ ) toward the heavier  $\text{RE}^{3+}$  ions (Fig. 4), because of the increasing repulsion experienced by the 4f electrons. The trends in the configuration interaction terms, i.e. the Trees parameters  $\alpha$ ,  $\beta$  and  $\gamma$ , are less regular, probably because they are less well defined. The Judd  $T^k$  parameters were in most cases fixed close to conventional values because the parameter values depend strongly on certain levels only. No large differences in the free ion parameters for the REOCl series could be found when compared to, for example, the  $\text{LaF}_3$  and  $\text{LaCl}_3$  series [24,35] indicating only weak dependence of the free ion interactions on the host matrix as the shielded position of the 4f orbitals suggests.

##### 4.2.2. Crystal field effects

Sufficient amounts of data are available at present on the c.f. parameters in the  $\text{RE}^{3+}$  series ( $\text{RE}^{3+} = \text{Pr}^{3+}, \text{Nd}^{3+}, \text{Sm}^{3+}, \text{Eu}^{3+}$  and  $\text{Tb}^{3+} - \text{Tm}^{3+}$ ) and a detailed comparison of the c.f. effect in the REOCl series [12–20] is thus possible. The simple reasoning based on the point charge model suggests that the c.f. effect should decrease with increasing nuclear charge, i.e. with increasing atomic number. This seems to hold up to the middle of the series (Fig. 5). However, beyond  $\text{Eu}^{3+}$  the c.f. effect regains

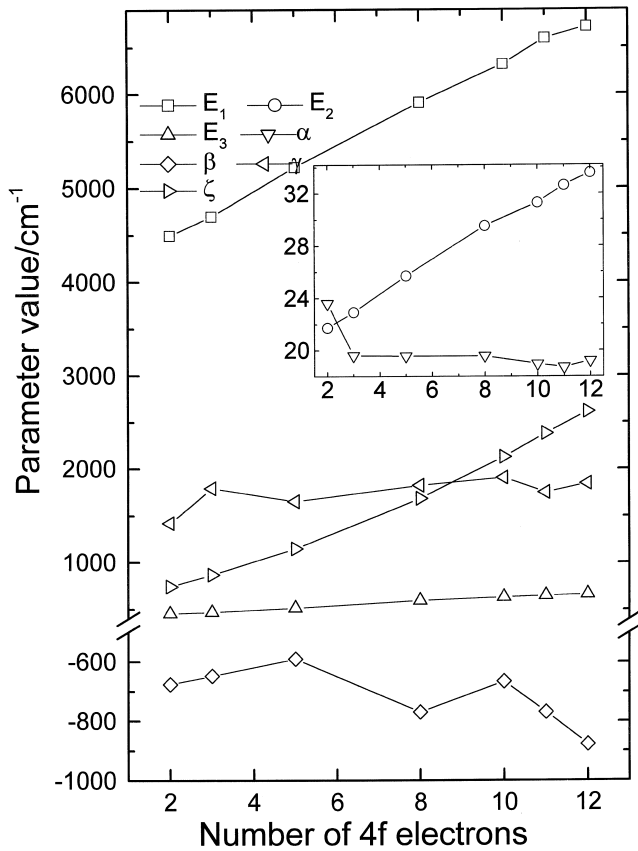


Fig. 4. Evolution of the free ion parameter values in the REOCl series.

strength as shown by the second- and fourth-rank parameters. The discontinuity from  $\text{Eu}^{3+}$  to  $\text{Tb}^{3+}$  can be interpreted as an indication of the need to include two-electron operators in the c.f. Hamiltonian [36]. Since the number of the two-electron c.f. parameters is very high it is very difficult to verify in a reliable manner this hypothesis. It

has also been suggested that the position of the next closest excited configurations, for example the 5d one, may have an effect on this kind of evolution of the c.f. parameters. This behaviour has been found for a number of matrices [37], although only for a few RE series is the amount of data close to complete. At the moment, this experimental observation has no reliable explanation.

#### 4.3. Modified electrostatic point charge and simple overlap model calculations

According to the modified electrostatic point charge model the  $B_q^k$  c.f. parameters can be expressed as products between the host dependent lattice sums  $A_q^k$  and the radial integrals  $\langle r^k \rangle$  [26]. As expected, all the  $\langle r^k \rangle$  values [28] decrease strongly toward the end of the RE series. However, when the correction factors  $\sigma_k$  and  $\tau$  are applied, the corrected  $\langle r^2 \rangle$  value in fact increases after a local minimum at  $\text{Gd}^{3+}$  which complicates the conclusions.

The calculation of the  $A_q^k$  lattice sums revealed that these values depend strongly on the coordination of the rare earth to oxygens. The RE–O sublattice makes up more than 60 and 85% of the  $A_0^2$  and  $A_q^k$  ( $k=4, 6$ ) values, respectively. The strong influence is most likely due to the short covalent RE–O bonds within the (REO) complex cation and results in the similarity of the energy level schemes and luminescence spectra of the tetragonal RE oxycompounds [38]. These similarities have been called the ‘fingerprint’ of this type of compounds [39].

The absolute  $A_q^k$  values increase quite linearly along with the increasing number of the 4f electrons (Fig. 6) though slight deviations can be observed for  $\text{CeOCl}$  and  $\text{PrOCl}$  as well as for  $\text{TbOCl}$ . These deviations underline the extreme sensitivity of the  $A_q^k$  values — especially  $A_0^2$  — on the structural data. It should be noted that the

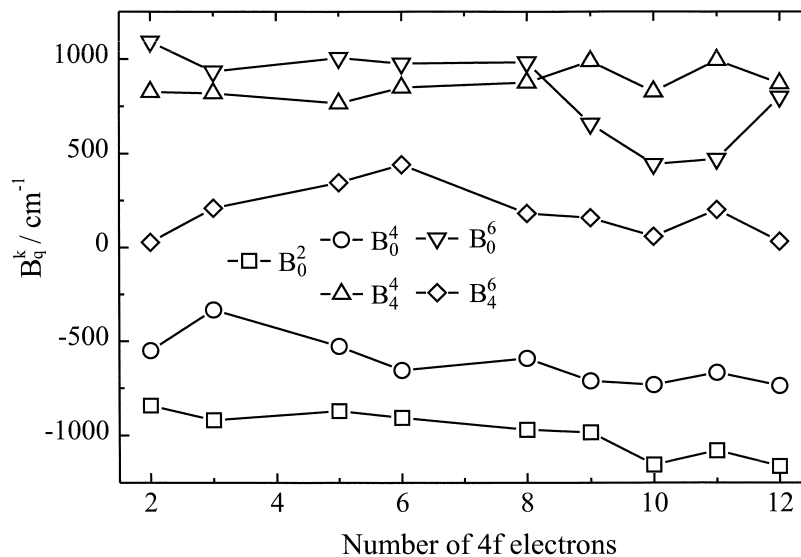


Fig. 5. Evolution of the experimental c.f. parameter values in the REOCl series.

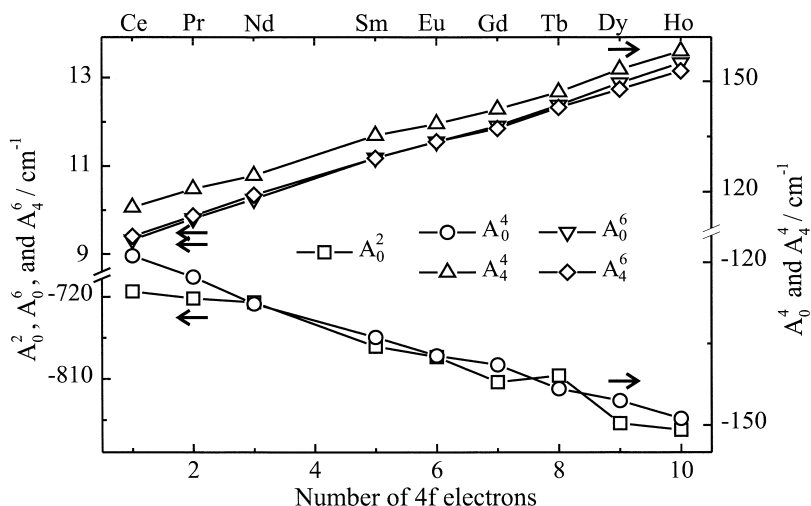


Fig. 6. Evolution of the PCEM  $A_q^k$  parameter values in the REOCl series.

evolution of the  $A_q^k$  values is the reverse of that usually expected for the point charge c.f. parameters. However, the decrease in the  $\langle r^4 \rangle$  and  $\langle r^6 \rangle$  values together with the shielding and expansion factors more than compensates for the increase in the  $A_q^k$  ( $k = 4, 6$ ) values, thus reproducing the expected decreasing trend. The PCEM  $B_0^2$  value shows much more complex behaviour in the RE series.

The Simple Overlap Model (SOM) takes into account only the ligands in the first coordination sphere around the  $RE^{3+}$  ion [31]. From the PCEM calculations it was found that the fourth- and sixth-order c.f. parameter values (or lattice sums) converge rapidly when the number of ions included in the calculations is increased.

Accordingly, the magnitude and evolution of the fourth- and sixth-rank parameters in the RE series are rather similar irrespective of the model used to calculate them. The differences may well be due to the different effective

charges used for the anions taking into account the inherent strong influence of the charges. Moreover, the SOM results were found to be very sensitive to the overlap parameter value,  $\rho$ . The  $B_q^k$  values increased strongly when  $\rho$  increased beyond 0.05.

The  $B_0^2$  value is an exception to the similarity between the PCEM and SOM sets of c.f. parameters (Fig. 7). The magnitude and evolution of these two sets of  $B_0^2$  parameters are clearly opposite to each other, as might be predicted from the slow and oscillating convergence of the  $A_0^2$  parameter. It is clear also that the farther lying ions should be included in the SOM calculations in order to reproduce the evolution of all the  $B_q^k$  parameters in the RE series — at least in the REOCl series.

Because of the similarities between the PCEM and SOM sets of the  $B_q^4$  and  $B_q^6$  parameter values and the resemblance of the evolution in the RE series between the

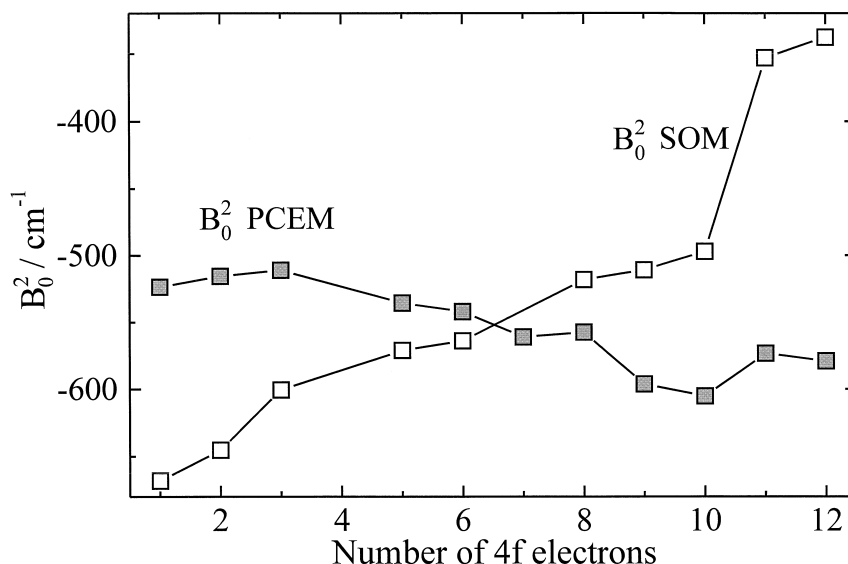


Fig. 7. Comparison between the PCEM and SOM  $B_0^2$  parameter values in the REOCl series.

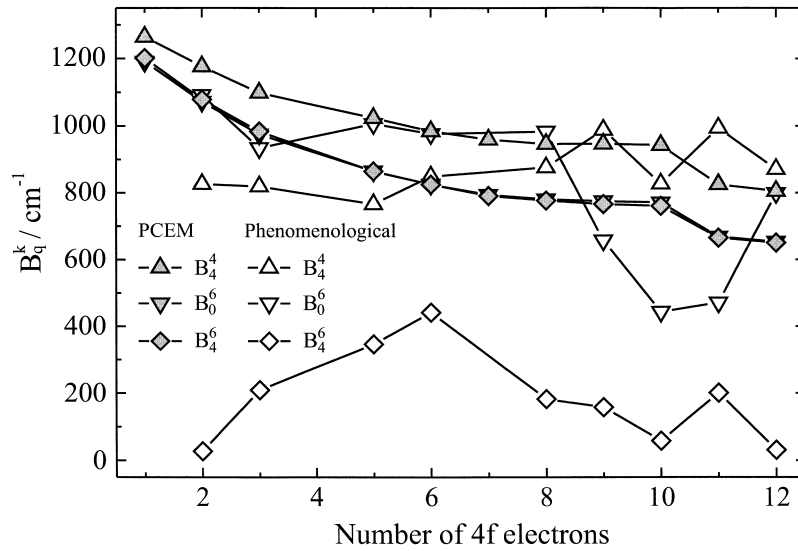


Fig. 8. Comparison between the PCEM and phenomenological  $B_4^4$ ,  $B_0^6$  and  $B_4^6$  parameter values in the REOCl series.

phenomenological and PCEM values of the  $B_0^2$  parameter, the comparison between the calculated and phenomenological parameter sets is carried out with the PCEM parameter set. The magnitude and evolution of the experimental and calculated sets of the  $B_4^4$  and  $B_0^6$  parameters are very similar (Fig. 8). The agreement for the  $B_4^6$  parameter sets is poor which may be due to the fact that this parameter is the least well determined experimentally since this parameter involves mainly the splitting between the levels labelled with the irreducible representations  $B_1$  and  $B_2$ . The observation of these levels is difficult because most transitions to/from these levels are forbidden by the group theoretical selection rules for the  $C_{4v}$  symmetry of the  $\text{RE}^{3+}$  site in RE oxchlorides. The magnitudes of the

remaining two parameter ( $B_0^2$ ,  $B_0^4$ ) sets (Fig. 9) are similar, but the trend in the REOCl series is opposite for the  $B_0^4$  parameter.

#### 4.4. Paramagnetic susceptibility

The average magnetic susceptibilities of the polycrystalline rare earth oxchlorides (REOCl, RE = Ce, Pr, Nd, Sm, Tb, Dy and Ho) were measured between 2 and 200–300 K. The curves for most REOCl samples follow the Curie–Weiss behaviour down to low temperatures (<20 K). TbOCl, SmOCl and DyOCl show additional antiferromagnetic ordering at 4, 8 and 11 K, respectively.

Since the wave functions and energies of the  $4f^N$  levels

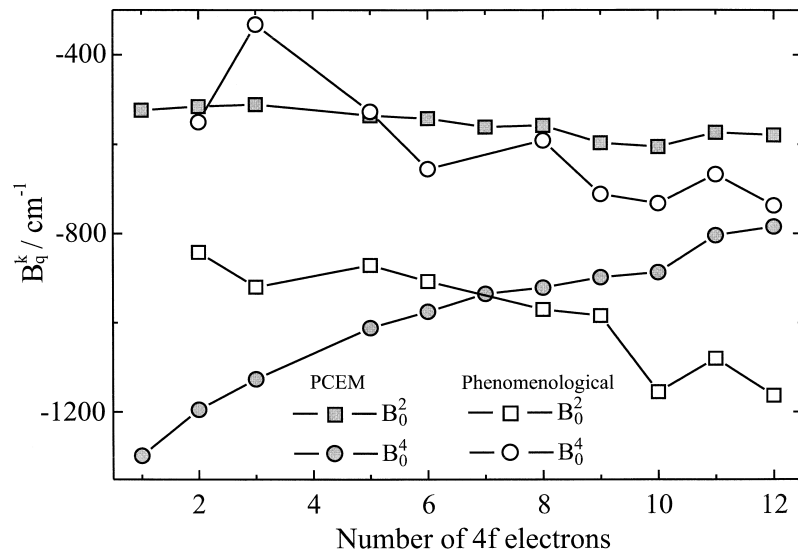


Fig. 9. Comparison between the PCEM and phenomenological  $B_0^2$  and  $B_0^4$  parameter values in the REOCl series.



are known, properties of the  $\text{RE}^{3+}$  ions other than the spectroscopic ones can be calculated. Such properties include the evolution of the paramagnetic susceptibility as a function of temperature. In the REOCl series, the data for calculations were obtained from the phenomenological modelling of the energy level schemes of the  $4f^N$  electron configurations. The experimental data could be reproduced well by the calculations, as shown by example for PrOCl (Fig. 10).

The optical data used in the calculations were determined mainly at 10 K. As a result, at high temperatures, the expansion of the crystal lattice which modifies the c.f. effect caused disagreement between the calculated and experimental paramagnetic susceptibilities. This disagreement increases with increasing temperature which may prove its origin. Further quantitative work on this phenomenon is currently under way with the NdOF system [40].

The deviation of the paramagnetic susceptibility of PrOCl from the Curie–Weiss behaviour at low temperature could be considered to result from the c.f. effect. Unfortunately, the observation of this low-temperature c.f. effect was hidden for several  $\text{RE}^{3+}$  ions because of the antiferromagnetic ordering below 20 K. The absolute temperature calculated for the c.f. effect to take place is not correct because the calculated c.f. splitting of the ground level does not match perfectly the experimental one. This is due to the inclusion of the higher energy levels in the simulation of the spectroscopic data which distorts the energies and wave functions of the lower levels which determine the paramagnetic susceptibility. When the effect of the configuration interaction terms is adequately known and taken into account, with the inclusion of the minor components in the Hamiltonian, the simulation of both the

higher energy level structure and the ground level might be enhanced.

## 5. Conclusions

The determination (or even the refinement) of the crystal structure of an isomorphous series of compounds such as RE oxychlorides (REOCl, RE=La–Ho and Y, excluding Pm) requires utmost care to exclude and/or compensate for the experimental artifacts. With the inclusion of the corrections for the microabsorption and preferred orientation, coherent and reliable structure data were obtained for use in the theoretical calculations of the  $4f^N$  energy level schemes in the  $\text{RE}^{3+}$  ions. The phenomenological simulations based on the UV–visible–NIR absorption and visible luminescence spectra were successfully carried out using a model which simultaneously accounted for the free ion and c.f. effects and used untruncated sets of the wave functions. The simulations involved up to 195 levels and generally yielded RMS deviations less than  $20 \text{ cm}^{-1}$ . Further work is in progress to include the minor configuration interaction terms and to improve the simulation of the higher energy level structure.

The structural data were used as inputs for the modified electrostatic point charge and simple overlap model calculations to reproduce the  $4f^N$  energy level schemes in the  $\text{RE}^{3+}$  ions in REOCl. The modified PCEM results underline the importance of the  $(\text{REO})_n^{n+}$  complex cation in determining the energy level schemes and the luminescence spectra of the RE oxychlorides. The SOM model, compensating for the inadequacies of the PCEM model to account for the covalence effect, emphasized the impor-

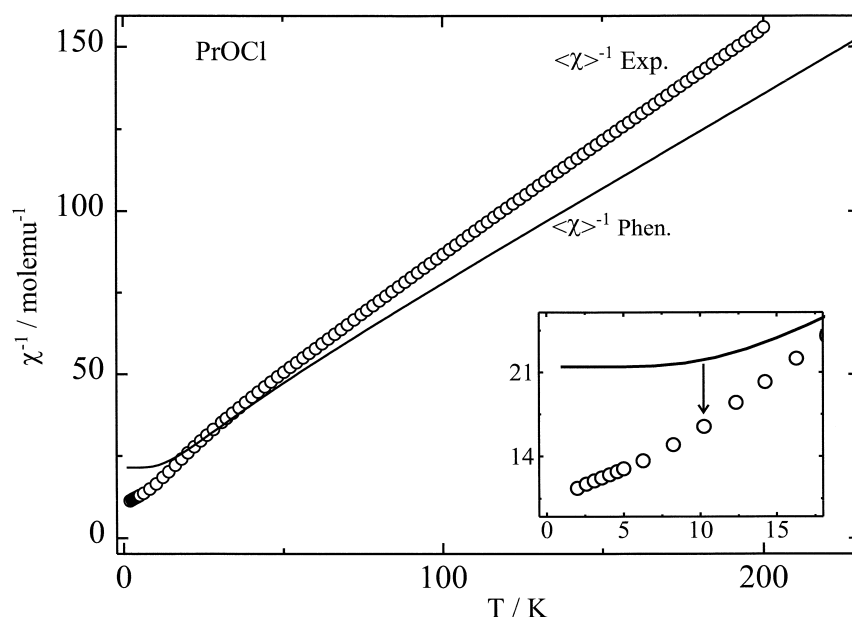


Fig. 10. Temperature dependence of the magnetic susceptibility of PrOCl.

tance of the overlap between metal and ligand wave functions. In general, the PCEM results reproduced the phenomenological data slightly better; in particular, the evolution of the second-order parameters behaved much better in the REOCl series.

The paramagnetic susceptibility of the RE<sup>3+</sup> ions as a function of temperature could be calculated successfully using the wave functions and energies obtained from the phenomenological modelling of the energy level schemes of the 4f<sup>N</sup> levels. Moreover, the experimental data could be reproduced well using the calculations, and the deviation from the Curie–Weiss behaviour at low temperature was concluded to result from the c.f. effect. Further work is in progress to correct the distortions of the energies and the wave functions of the lower levels caused by the inclusion of the higher energy levels in the simulation of the spectroscopic data.

### Acknowledgements

Financial support from the Academy of Finland, the Graduate School of Materials Research (Turku) and the University of Turku is acknowledged. Some of the rare earth oxides used were provided by Rhodia S.A. (Aubervilliers). The contributions of several researchers at UMR 7574 (CNRS, ENSCP, Paris, France), the Departamento de Química Inorgánica I, (Universidad Complutense, Madrid, Spain), the Institute of Low Temperature and Structure Research (Polish Academy of Sciences, Wrocław, Poland), the Department of Chemistry (University of Jyväskylä, Jyväskylä, Finland) and the Department of Chemistry (University of Turku, Turku, Finland) to this work are most gratefully acknowledged.

### References

- [1] G. Blasse, A. Bril, *J. Chem. Phys.* 46 (1967) 2579.
- [2] L.G. Sillén, A.-L. Nylander, *Svensk Kem. Tidskr.* 53 (1941) 367.
- [3] L.H. Brixner, E.P. Moore, *Acta Cryst. Ser. C* 39 (1983) 1316.
- [4] D.H. Templeton, C.H. Dauben, *J. Am. Chem. Soc.* 75 (1953) 6069.
- [5] M. Wolczyr, L. Kepinski, *J. Solid State Chem.* 99 (1992) 409.
- [6] W.H. Zachariasen, *Acta Crystallogr.* 2 (1949) 388.
- [7] G. Meyer, T. Schleid, *Z. Anorg. Allg. Chem.* 533 (1986) 181.
- [8] H. Bärnighausen, G. Brauer, N. Schultz, *Z. Anorg. Allg. Chem.* 338 (1965) 250.
- [9] J. Hölsä, E. Säilynoja, K. Koski, H. Rahiala, J. Valkonen, *Powder Diffr.* 11 (1996) 129.
- [10] F. Weigel, V. Wishnevsky, *Chem. Ber.* 102 (1969) 5.
- [11] G. Meyer, T. Staffel, *Z. Anorg. Allg. Chem.* 532 (1986) 31.
- [12] E. Antic-Fidancev, J. Hölsä, M. Lemaître-Blaise, P. Porcher, *J. Chem. Soc.: Faraday Trans.* 87 (1991) 3625.
- [13] L. Beaury, Ph.D. Thesis, Université de Paris-Sud, Orsay, France, 1988, p. 128.
- [14] J. Hölsä, R.-J. Lamminmäki, P. Porcher, 1998, unpubl.
- [15] J. Hölsä, P. Porcher, *J. Chem. Phys.* 75 (1981) 2108.
- [16] J. Hölsä, R.-J. Lamminmäki, P. Porcher, H.F. Brito, *Quim. Nova* 19 (1996) 237.
- [17] J. Hölsä, R.-J. Lamminmäki, P. Porcher, *J. Alloys Comp.* 275–277 (1998) 398.
- [18] J. Hölsä, R.-J. Lamminmäki, P. Porcher, 1997, unpubl.
- [19] J. Hölsä, E. Säilynoja, R.-J. Lamminmäki, P. Dereń, W. Stręk, P. Porcher, *J. Chem. Soc.: Faraday Trans.* 93 (1997) 2241.
- [20] J. Hölsä, R.-J. Lamminmäki, E. Antic-Fidancev, M. Lemaître-Blaise, P. Porcher, *J. Phys.: Condens. Matter* 7 (1995) 5127.
- [21] J. Hölsä, L. Niinistö, *Thermochim. Acta* 37 (1980) 155.
- [22] P. Porcher, Computer Programs REEL and IMAGE for the Simulation of d<sup>N</sup> and f<sup>N</sup> Configurations Involving the Real and Complex Crystal Field Parameters, Meudon, France, 1989, unpubl.
- [23] B.G. Wybourne, *Spectroscopic Properties of Rare Earths*, Interscience, New York, 1965, Chapter 6.
- [24] W.T. Carnall, G.L. Goodman, K. Rajnak, R.S. Rana, *J. Chem. Phys.* 90 (1989) 3443.
- [25] J. van Vleck, *J. Appl. Phys.* 39 (1968) 365.
- [26] R.P. Leavitt, C.A. Morrison, D.E. Wortman, Report TR-1673, Harry Diamond Laboratories, Adelphi, MD, 1975.
- [27] P. Porcher, Program Somaille for Point Charge Lattice Sum Calculations, CNRS, Meudon, France, 1987, unpubl.
- [28] A.J. Freeman, J.P. Desclaux, *J. Magn. Magn. Mater.* 12 (1979) 11.
- [29] F. Jollet, C. Noguera, N. Thorntat, M. Gautier, P. Duraud, *Phys. Rev. B* 42 (1990) 7587.
- [30] O.L. Malta, *Chem. Phys. Lett.* 87 (1982) 27.
- [31] P. Porcher, M. Couto dos Santos, O. Malta, *Phys. Chem. Chem. Phys.* 1 (1999) 397.
- [32] J. Strähle, *Z. Anorg. Allg. Chem.* 402 (1973) 47.
- [33] R.D. Shannon, *Acta Crystallogr.* A32 (1976) 751.
- [34] J. Hölsä, R.-J. Lamminmäki, P. Porcher, 1999, unpubl.
- [35] C.K. Jayasankar, F.S. Richardson, *J. Less-Common Met.* 148 (1989) 289.
- [36] M.F. Reid, *J. Chem. Phys.* 87 (1987) 2875.
- [37] C. Görrler-Walrand, K. Binnemans, Rationalization of crystal-field parametrization, in: K.A. Gschneidner Jr., L. Eyring (Eds.), *Handbook of Physics and Chemistry of Rare Earths*, Vol. 23, Elsevier, Amsterdam, 1996, Chapter 155.
- [38] J. Hölsä, T. Turkki, *Thermochim. Acta* 190 (1991) 335.
- [39] P. Porcher, P. Caro, *J. Less-Common Met.* 93 (1983) 151.
- [40] M. Lastusaari, J. Hölsä, J. Rodriguez-Carvajal, L. Beaury, J. Derouet, XVIIIth Intl. Union Cryst. Congr., August 4–13, 1999, Glasgow, UK, p. 241.